SUPPLEMENTAL MATERIAL

Table S1. Mouse MAbs used in this study.

MAb	Subclass	Target (cluster)	Reference
PB10	IgG2b	RTA (I)	[1]
WECB2	IgG1		[3]
SyH7	IgG1	RTA (II)	[1]
PA1	IgG1		[3]
IB2	IgG1	RTA (III)	[3]
JD4	IgG1		[3]
8B3	IgG1	RTB	[5]
LC5	IgG1		[6]
8A1	IgG1		[6]
24B11	IgG1		[6]
SyH3	IgG1		[6]
MH3	IgG1		[6]

[1] O'Hara JM, Neal LM, McCarthy EA, Kasten-Jolly JA, Brey RN, 3rd, Mantis NJ. Folding domains within the ricin toxin A subunit as targets of protective antibodies. Vaccine. 2010;28:7035-46.

[2] Lemley PV, Amanatides P, Wright DC. Identification and characterization of a monoclonal antibody that neutralizes ricin toxicity in vitro and in vivo. Hybridoma. 1994;13:417-21.

[3] O'Hara JM, Kasten-Jolly JC, Reynolds CE, Mantis NJ. Localization of non-linear neutralizing B cell epitopes on ricin toxin's enzymatic subunit (RTA). Immunol Lett. 2014;158:7-13.

[4] Neal LM, O'Hara J, Brey RN, 3rd, Mantis NJ. A monoclonal immunoglobulin G antibody directed against an immunodominant linear epitope on the ricin A chain confers systemic and mucosal immunity to ricin. Infect Immun. 2010;78:552-61.

[5] Yermakova A, Mantis NJ. Protective immunity to ricin toxin conferred by antibodies against the toxin's binding subunit (RTB). Vaccine. 2011;29:7925-35.

[6] Rong Y, Van Slyke G, Vance DJ, Westfall J, Ehrbar D, Mantis NJ. Spatial location of neutralizing and non-neutralizing B cell epitopes on domain 1 of ricin toxin's binding subunit. PLoS One. 2017;12:e0180999.

Table S2. Commercial primary antibody information for flow cytometry.

Target	Dilution	Source	Conjugate	Vendor
CD206	1:800	Mouse	PE	BioLegend
CD206	1:200	Rat	FITC	BioLegend
CD45	1:4000	Mouse	PE	BioLegend
CD45	1:1600	Mouse	FITC	BioLegend
CD146	1:50	Mouse	FITC	Abcam
CD146	1:2000	Rat	PE	BD Pharmingen
F4/80	1:1200	Rat	AF647	BD Pharmingen
CD11b	1:4000	Rat	PE	BD Biosciences

Supplemental Figure Legends

Figure S1. Flow cytometric analysis of murine KCs and LSECs. Flow cytometric analysis of positively-selected mouse KCs (panels **A, C, E**) and LSECs (panels **B, D, F**) stained for (**A, B**) F4/80 (y-axis) and CD146 (x-axis), (**C, D**) CD45 (y-axis) and CD146 (x-axis), and (**E, F**) propidium iodide (y-axis) for cell viability. Panel B indicates that the LSEC preparation is contaminated with a fraction (~7-8%) of KCs. Panel D demonstrates LSECs consist of two subpopulations (circled): subset 1 that is $CD146^-/CD45^{high}$ (~64% cells) and subset 2 that is $CD146^+/CD45^+$ (~20% cells). The third population in panel D is made up of contaminating KCs (~10%).

Figure S2. Mannose receptor (CD206) expression and the ability to inhibit cellular attachment of ricin toxin with lactose and α-mannan. (Panel A) KCs, J774E and LSECs cell suspensions stained with anti-CD206 (y-axis) and anti-CD45 (x-axis) and examined by flow cytometry. The plots show that KCs and J774E cells uniformly express the mannose receptor (CD206). The $CD146^+/CD45^+$ LSECs (subset 2) also express CD206, whilst the $CD146^-/CD45^{hi}$ (subset 1) does not. (**Panel B**) KCs, J774E and LSECs cell suspensions at 4ºC were incubated with FITC-conjugated ricin toxin without or with mannan (1 mg/ml), lactose (0.1 M) or a combination of both mannan and lactose, and then subjected to flow cytometry. Ricin toxin attachment to KCs and LSECs was almost completely blocked by lactose, but very little by mannan, demonstrating that toxin attachment is mediated by RTB even though actual toxicity of KCs and LSECs is mannose-sensitive and therefore mediated by the mannose receptor or another C-type lectin (see main text).

Figure S3. Neutralizing activity of anti-RTB MAbs in the KC cytotoxicity assay. Freshly isolated KCs were seeded into 96-well microtiter plates and then treated with ricin plus indicated amount of anti-RTB MAbs for 18 h, as described in the main text. MAbs SylH3 and 24B11 afforded moderate toxin-neutralizing activity, 8B3 and MH3 provided weak toxin-neutralizing activity, while 8A1 and LC5 were ineffective.

Figure S4. Co-administration of SylH3 with ricin toxin prevents KC depletion. Groups of mice were challenged by the IV route with saline (top), ricin toxin (middle) or ricin toxin plus SylH3, as described in the Materials and Methods. Eighteen hours later, liver cell suspensions were analyzed by flow cytometry for KC populations [F4/80 (*y-axis*) and CD45 (*x-axis*)]. Alternatively, formalin-fixed liver tissue sections were subjected to IHC with anti-F4/80 antibody or anti-cleaved caspase 3 antibodies. F4/80 (middle column) or cleaved caspase-3 (right column) positive cells are denoted with arrows colored red or black for contrast, depending on the panel. Ricin treatment alone resulted in a near complete depletion of KCs (<1%) and a corresponding increase in cells positive for activated caspase-3. The addition of SylH3 resulted in the retention of KCs numbers and reduction in the number of cells positive for activated caspase-3.

Figure S5. Cocktails of four anti-RTA MAbs, each targeting a specific RTA cluster, necessary to achieve complete ricin toxin neutralization in ex vivo primary LSECs. LSECs were seeded in 96 well microtiter plates and then treated with indicated combinations of (**A**) two, (**B**) three anti-RTA or (**C**) the various combinations of two, three or four MAbs. Cell viability was normalized to LSECs treated with vehicle (saline), as described in the Materials and Methods. Each data point represents the average (with corresponding standard deviations) of three independent experiments.

Figure S6. Antisera from RiVax vaccinated mice protects LSECs from ricin induced killing. Freshly isolated (A) KCs, (B) J774E cells or (C) LSECs were seeded into 96-well microtiter plates and then treated with ricin plus indicated dilution of pooled anti-sera from RiVax immunized mice, as described in the Materials and Methods. Cell viability was assessed 18 later. A single representative experiment done in triplicate is shown.

Figure S1

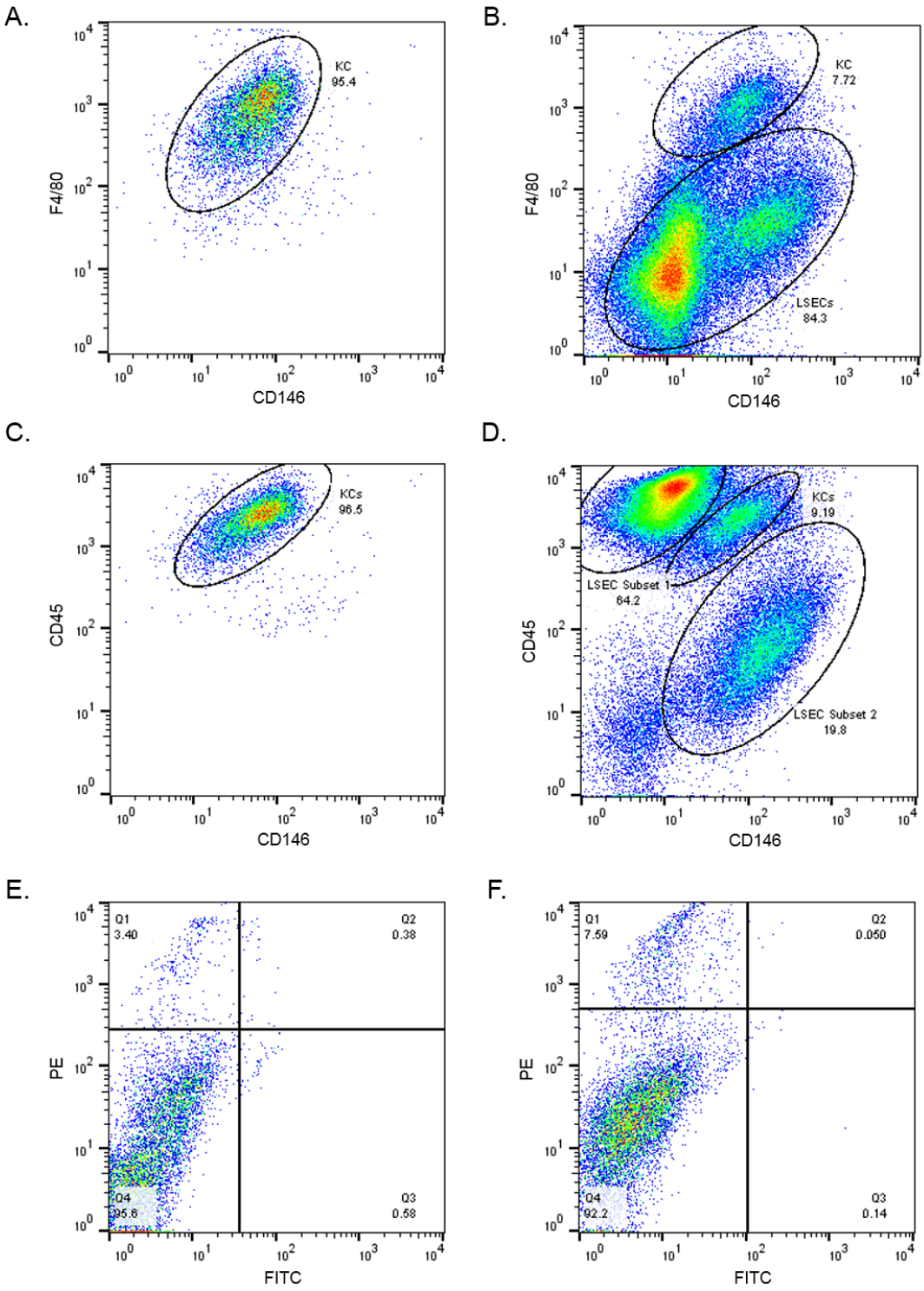
A.
KC
95.4
F4/80
CD146
B.
KC
7.72
LSECs
84.3
F4/80
CD146
C.
KCs
96.5
CD45
CD146
D.
KCs
9.19
LSEC Subset 1
64.2
LSEC Subset 2
19.8
CD45
CD146
E.
Q1
3.40
Q2
0.38
Q4
95.6
Q3
0.58
PE
FITC
F.
Q1
7.59
Q2
0.050
Q4
92.2
Q3
0.14
PE
FITC

Figure S2

A.

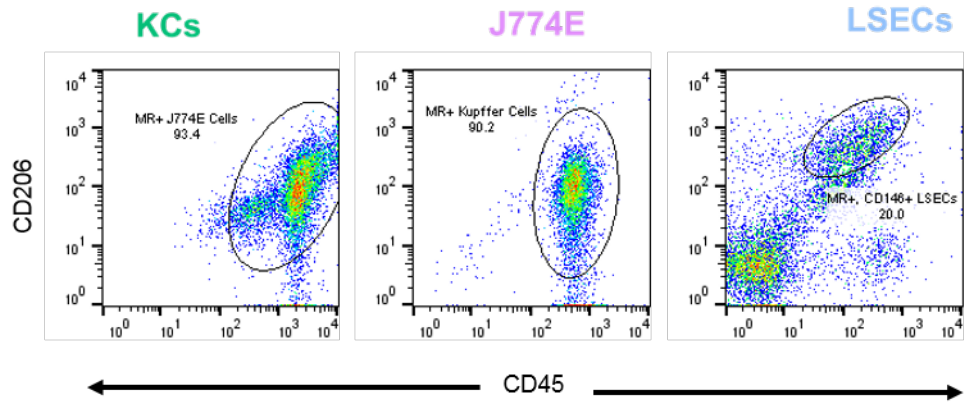
KCs
J774E
LSECs
CD206
MR+ J774E Cells
93.4
MR+ Kupffer Cells
90.2
MR+, CD146+ LSECs
20.0
CD45

B.

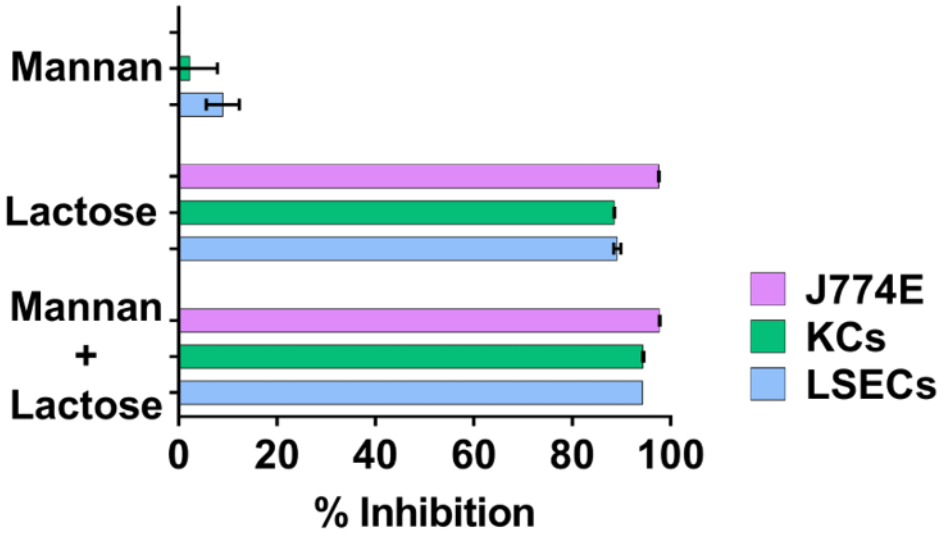
Mannan
Lactose
Mannan
+
Lactose
0
20
40
60
80
100
% Inhibition
J774E
KCs
LSECs

Figure S3

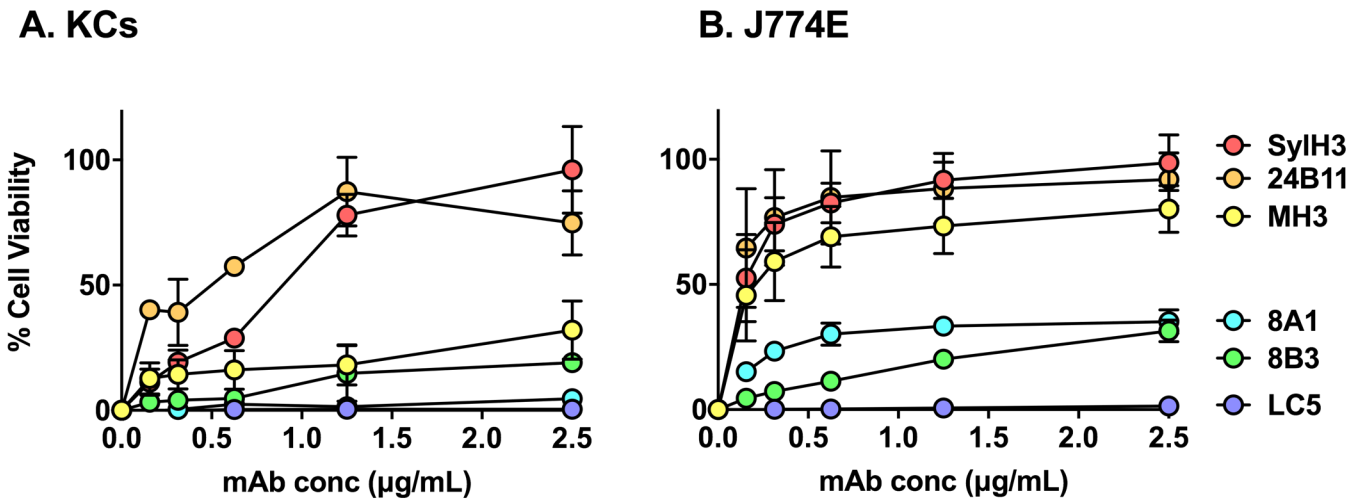
A. KCs
B. J774E
% Cell Viability
100
50
0
0.0
0.5
1.0
1.5
2.0
2.5
mAb conc (µg/mL)
SylH3
24B11
MH3
8A1
8B3
LC5

Figure S4

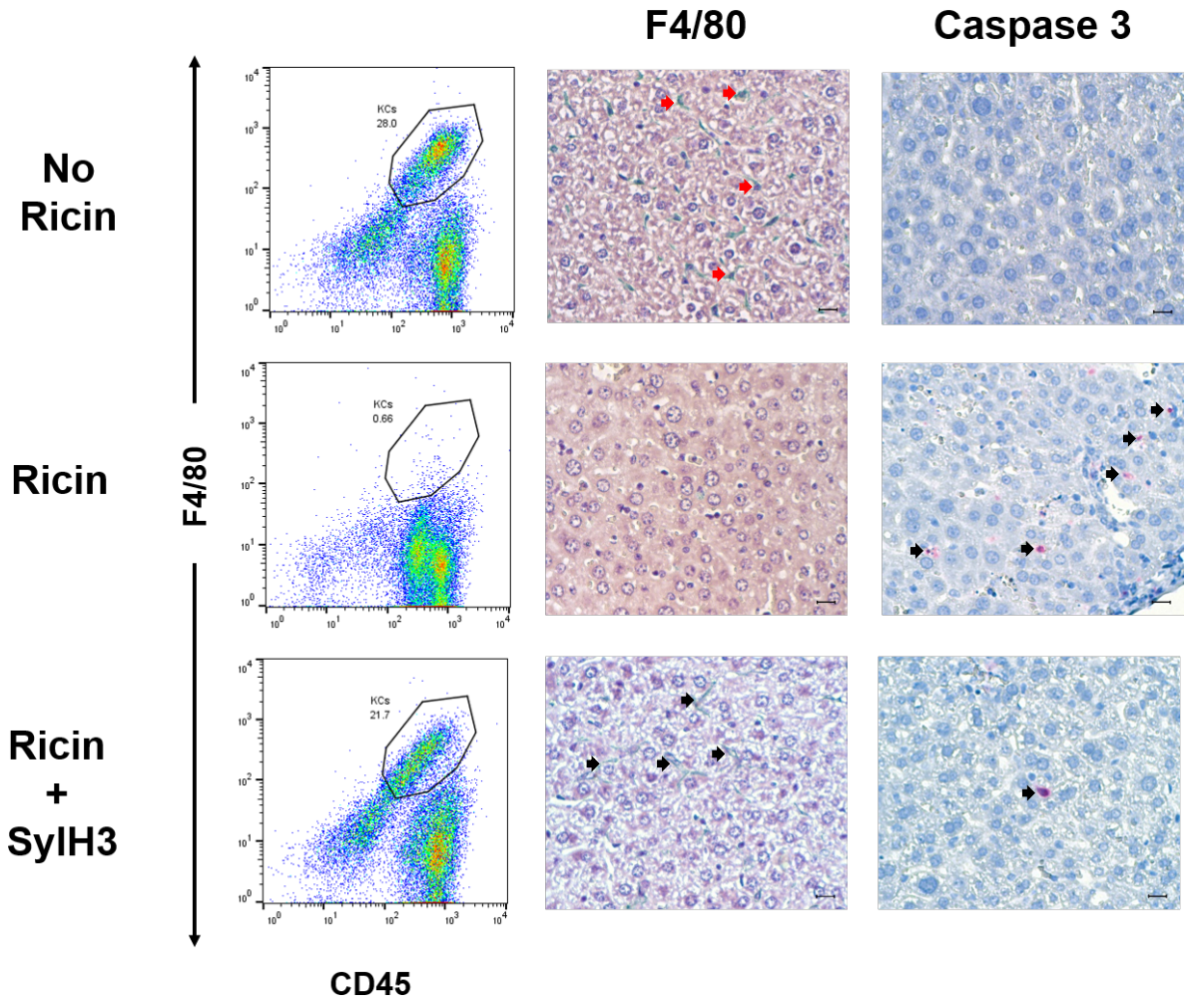
F4/80
Caspase 3
No Ricin
Ricin
Ricin + SylH3
F4/80
CD45
KCs 28.0
KCs 0.66
KCs 21.7

Figure S5

A.

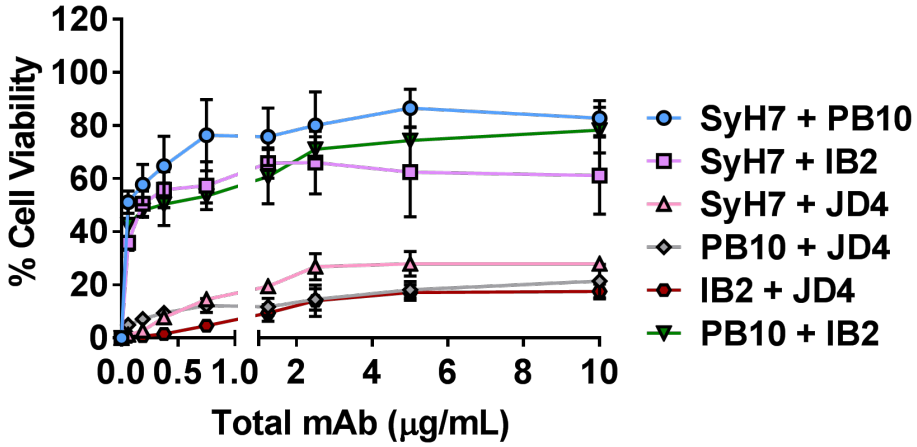

B.

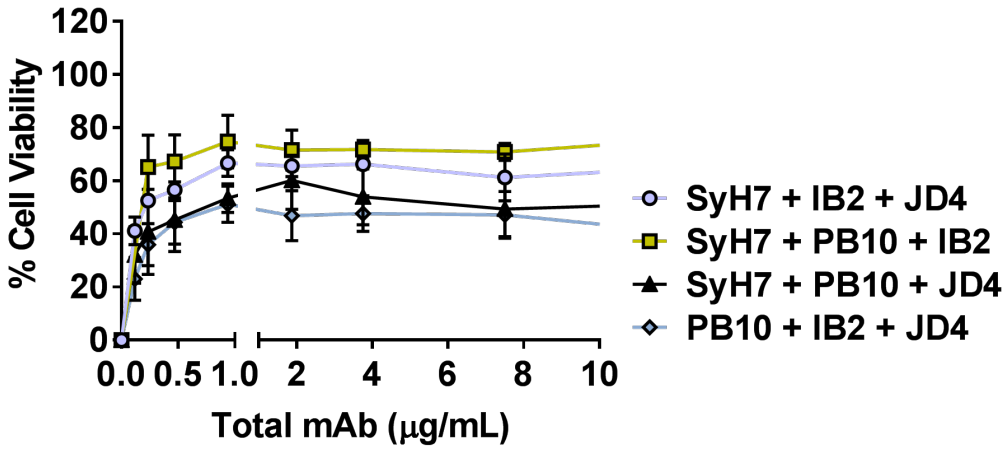

C.

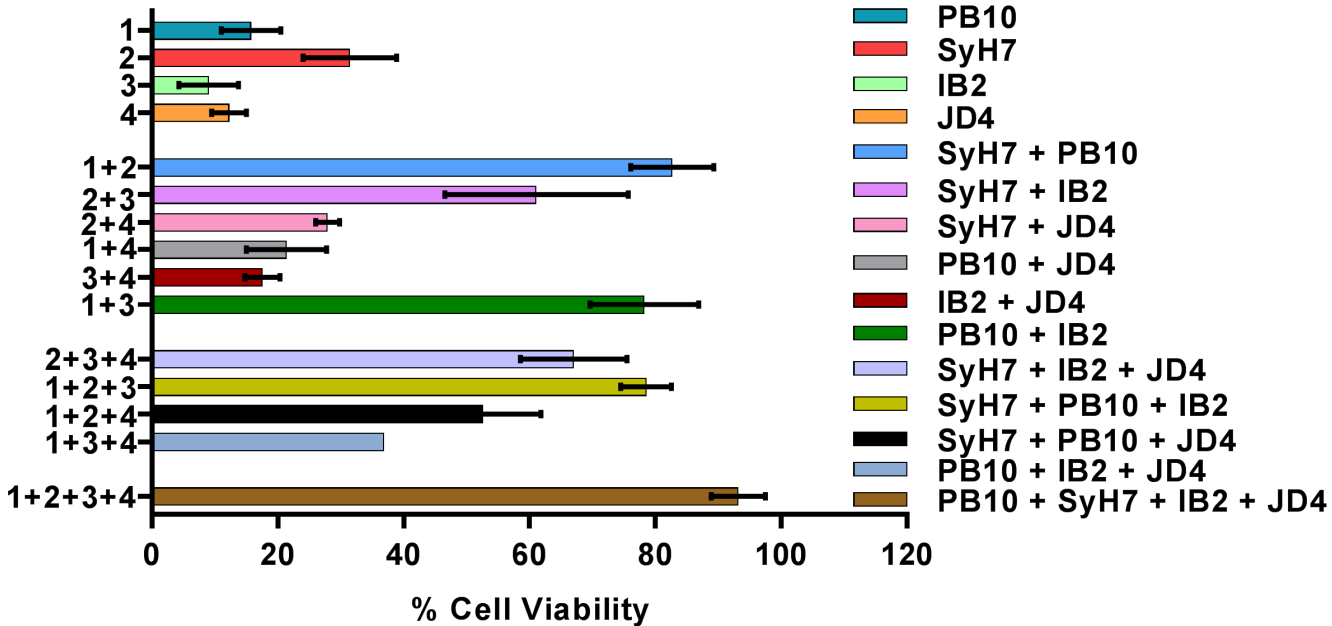

Figure S6

A. KCs

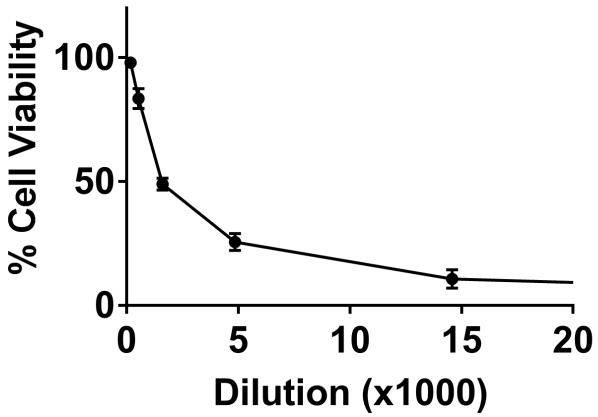

B. J774E

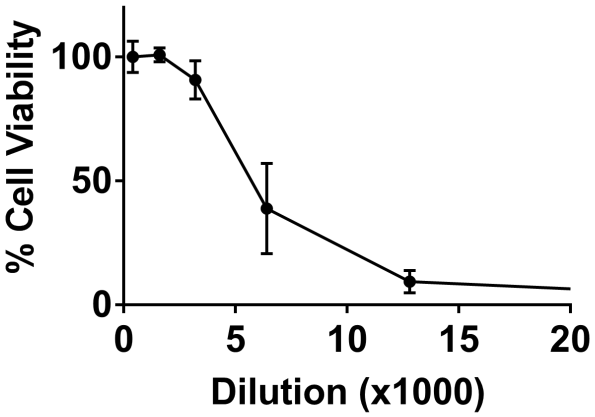

C. LSECs